Twofold surface of the decagonal Al-Cu-Co quasicrystal

T. Duguet,[1] B. Ünal,[2] M. C. de Weerd,[1] J. Ledieu,[1] R. A. Ribeiro,[3,*] P. C. Canfield,[3] S. Deloudi,[4] W. Steurer,[4] C. J. Jenks,[2]
J. M. Dubois,[1] V. Fournée,[1] and P. A. Thiel[2]

[1]*Institut Jean Lamour, UMR 7198 CNRS, Nancy-Université, UPV-Metz, Ecole des Mines de Nancy, Parc de Saurupt, CS14234,*
F-54042 Nancy, France
[2]*Ames Laboratory and Departments of Chemistry and Materials Sciences and Engineering, Iowa State University,*
Ames, Iowa 50011, USA
[3]*Ames Laboratory and Department of Physics and Astronomy, Iowa State University, Ames, Iowa 50011, USA*
[4]*Laboratory of Crystallography, ETH Zurich, Wolfgang-Pauli-Strasse 10, 8093 Zurich, Switzerland*

We have investigated the atomic structure of the twofold surface of the decagonal Al-Cu-Co quasicrystal using scanning tunneling microscopy and low-energy electron diffraction. We have found that most of the surface features can be interpreted using the bulk-structure model proposed by Deloudi and Steurer (S. Deloudi, Ph.D. thesis, ETH, Zürich, 2008). The surface consists of terraces separated by steps of various heights. Step heights and steps sequences match with the thickness and the stacking sequence of blocks of layers separated by gaps in the model. These blocks of layers define possible surface terminations consisting of periodic atomic rows which are aperiodically stacked. These surface terminations are dense ($\sim$10 at./nm^2) and are of three types. The first two types are pure or almost pure Al while the third one contains 30–40 at. % of transition-metal atoms. Experimentally, we observe three different types of fine structures on terraces, which can be interpreted using the three possible types of bulk terminations. Terraces containing transition metals exhibit a strong bias dependency and present a doubling of the basic 0.42 nm periodicity, in agreement with the 0.84 nm superstructure of the bulk. In addition, a high density of interlayer phason defects is observed on this surface that could contribute to the stabilization of this system through configurational entropy associated with phason disorder.

I. INTRODUCTION

Long-range quasiperiodic order has a strong effect on the physical properties of metallic alloys. A direct illustration of this effect is the strong anisotropy measured in the transport properties of decagonal (*d*) quasicrystals such as *d*-Al-Ni-Co or *d*-Al-Cu-Co.[1,2] These alloys are quasiperiodic in two dimensions and periodic in the third dimension. The electrical resistivity is found to be metalliclike along the periodic axis, while the temperature coefficient is negative (i.e., nonmetallic) within the quasiperiodic plane. A strong anisotropy of the friction properties has also been measured on the twofold surface of a *d*-Al-Ni-Co phase using atomic force microscopy.[3,4] The friction force between the surface and the cantilever is found to be reduced by a factor of 8 when sliding along the quasiperiodic axis compared to the periodic one. The fact that both periodic and quasiperiodic directions coexist on twofold surfaces of decagonal quasicrystals makes them interesting systems. However, only a few studies of such surfaces have been reported so far and they are exclusively devoted to *d*-Al-Ni-Co quasicrystals.[5–7]

The first *d*-Al-Cu-Co phase was discovered in 1988.[8] The Al-Cu-Co phase diagram was investigated later in detail by Grushko.[9,10] The composition range of thermodynamic stability is found to shift and widen with increasing temperature. The stable decagonal phase can be found for chemical compositions ranging between $Al_{69}Co_{21}Cu_{10}$ and $Al_{62}Co_{14}Cu_{24}$. The temperature stability domain of the *d* phase has been determined for a composition of $Al_{65}Co_{17.5}Cu_{17.5}$ (i.e., close to our sample composition) and

ranges from 973 to 1350 K.[11] Single crystals of several millimeters in size have been grown successfully, either by slow cooling or Czochralski methods.[12–15] The structure of the phase has been investigated mainly by high-resolution transmission electron microscopy and x-ray diffraction. Here we use the bulk-structure model proposed by Deloudi and Steurer.[16] It has been derived within a systematic cluster-based modeling of Al-based decagonal phases with two- and four-layer periodicity and is based on single-crystal x-ray-diffraction analysis of a decagonal phase with composition $Al_{65}Cu_{20}Co_{15}$ using a Patterson analysis and subsequent least-squares refinement from Steurer and Kuo.[17] The space group of the crystal is $P10_5/mmc$ and the lattice parameter along the periodic axis is 0.408 nm. It is not possible to distinguish between Cu and Co atoms with x-ray diffraction; therefore, both Cu and Co are referred to as a generic transition metal (TM) in the following. Several variants of the model have been proposed, emphasizing the role of chemical order in the electronic structure and phase stability.[18–21] An overview of the various models can be found in Ref. 22. A section of the model is shown in Fig. 1, viewed perpendicular to the 10-fold axis. It consists of two fivefold symmetric quasiperiodic layers related by a 10_5 screw axis, leading to an overall 10-fold symmetry around the [00001] axis. The quasiperiodic planes can be described by an ideal Penrose tiling made up of acute and obtuse rhombic tiles characterized by angles of 36° and 72°, respectively. Large clusters of diameter $\sim$2 nm occupy the vertices of the Penrose tiling. The two inequivalent twofold axis [10000] and [001$\bar{1}$0] are indicated in Fig. 1.
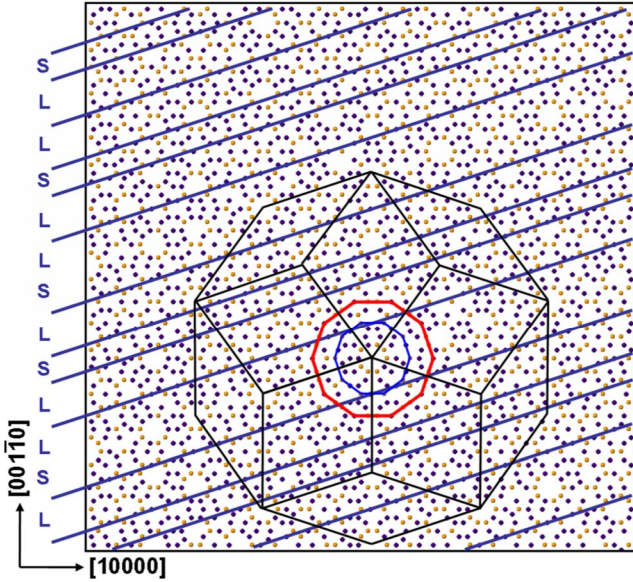
FIG. 1. (Color online) Atomic structure (10×10 nm^2) of the *d*-Al-Cu-Co quasicrystal in the tenfold plane according to the model by Deloudi and Steurer (Ref. 16). The grid indicates densely spaced atomic rows. These are inclined by 18° from the horizontal and correspond to a (10000) orientation. The spacing follows a Fibonacci sequence with $S = 0.475$ nm and $L = \tau S = 0.769$ nm. The dark (blue) and bright (orange) dots correspond to Al and TM atoms, respectively. An ideal Penrose tiling is superimposed. The edge of the rhombic tiles is 2.0 nm. The largest decagon decorating the Penrose tiling corresponds to the basic cluster unit.

The 10-fold surface of a *d*-Al$_{65}$Cu$_{15}$Co$_{20}$ alloy has been investigated by Kortan *et al.*[23] The scanning tunneling microscopy (STM) images were interpreted as a simple termination of the bulk quasiperiodic structure. They confirmed that the structure is described as the stacking of two basic planes having a pentagonal symmetry, rotated by 36° from each other and separated by a single step of about 0.2 nm. The in-plane structure could be interpreted using a pentagonal quasilattice. The twofold surface of the *d*-Al-Cu-Co quasicrystal has not been investigated yet but related studies of the twofold *d*-Al-Ni-Co have been reported.[5–7] These two alloys (*d*-Al-Cu-Co and *d*-Al-Ni-Co) have similar structures. It was found that the twofold *d*-Al-Ni-Co surface consists of terraces, separated by steps of heights 0.19, 0.47, 0.78, and 1.26 nm, and containing periodic atomic rows arranged aperiodically in the perpendicular direction. In addition, it appeared that the surfaces are preferentially Al terminated and their structure is in general agreement with bulk models.[7]

In this paper, we present a detailed study of the atomic structure of the twofold surface of a Al$_{63.2}$Co$_{19.5}$Cu$_{17.3}$ decagonal phase. The surface is investigated by low-energy electron diffraction (LEED) and STM. We show that most of the structural features observed experimentally can be interpreted using the bulk-structure model proposed by Deloudi and Steurer.[16] We also point out some differences between twofold surfaces of decagonal Al-Ni-Co and Al-Cu-Co quasicrystals.

II. EXPERIMENTAL DETAILS

Single crystals with composition Al$_{63.2}$Co$_{19.5}$Cu$_{17.3}$ were grown from the ternary melt by the slow-cooling method, as described by Ribeiro *et al.*[13] Grains have the shape of decagonal rods extending along the preferred growth direction, which corresponds to the periodic [00001] axis. Perpendicular to this direction, rods exhibit facets that are perpendicular to the ⟨10000⟩ twofold axes. The second set of inequivalent twofold axes is indexed as ⟨001$\bar{1}$0⟩ and point toward the edges formed by two adjacent facets. Therefore the normals to (001$\bar{1}$0) surfaces are rotated by 18° with respect to (10000) surface ones. Two samples were extracted from initial single grain and polished with diamond paste (1/4 μm) so as to exhibit a surface-oriented perpendicular to a [10000] twofold axis. The surface orientation was checked by back-Laue scattering. Both samples have a bulk periodicity of 0.84 nm, double of the basic 0.42 nm periodicity of decagonal phases. This is observed in selected area electron-diffraction (SAED) patterns along [001$\bar{1}$0] showing diffuse interlayer lines indicative for the 0.84 nm superstructure.[13] This 0.84 nm superstructure is however not observed in [10000] SAED image because of systematic extinction in the diffuse scattering due to the *c*-glide plane.

Two sets of experiments were performed using these two samples in two different UHV chambers, both having a base pressure in the low 10^{-11} mbar range. We will refer to the two samples as A1 and N1 in the following. In both cases, a clean surface was achieved by repeated cycles of Ar$^+$ sputtering (2 kV) and annealing (between 973 and 1073 K). The temperature was monitored by using an optical pyrometer (emissivity set to $\varepsilon = 0.35$). The surface structure was investigated by STM and LEED. STM experiments were carried out using an Omicron VT-STM and the images were analyzed using the WSXM software.[24] The reciprocal space in LEED measurements was calibrated using a clean Cu(111) surface as a reference sample.

III. EXPERIMENTS

The LEED pattern of the clean surface is shown in Fig. 2. The horizontal direction corresponds to the periodic [00001] axis. Diffraction spots are aligned along vertical lines corresponding to the quasiperiodic [001$\bar{1}$0] direction. The spots are slightly more elongated along the quasiperiodic direction than along the periodic direction. In addition, there is some diffuse scattering intensity in between the spots. This indicates a limited correlation length along the [001$\bar{1}$0] direction. This is consistent with phason disorder discussed later in the paper. The [00001] component of the *k* vectors is $\pm n \cdot$b, with *n* an integer and b$= 7.8$ nm^{-1}, corresponding to a periodicity of about 0.8 nm along the periodic direction. The diffraction spots are much sharper for even *n*, corresponding to the basic 0.4 nm periodicity observed in the bulk. The diffraction vectors of the spots appearing along the quasiperiodic direction can be expressed as $k = k_0 (m + n\tau)$ with (m, n) integers and $k_0 = 6.1$ nm^{-1}. These values are similar to those reported for the same [10000] twofold surface of the *d*-AlNiCo phase.[6] The weak 0.8 nm periodicity observed in the LEED pattern is consistent with the diffuse interlayer lines indicative for
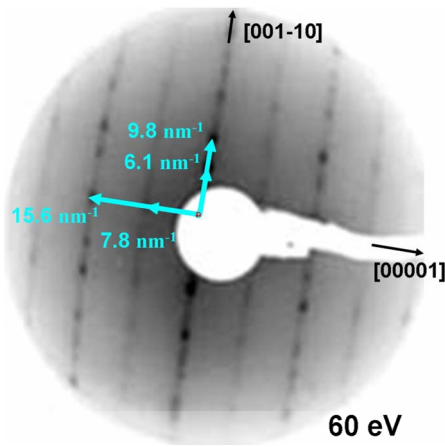
FIG. 2. (Color online) LEED pattern of the twofold d-AlCu-Co (10000) surface taken at 60 eV electron energy showing a periodic ordering along the [00001] direction and quasiperiodic ordering along the [001$\bar{1}$0] direction.

the 0.84 nm superstructure observed in SAED pattern on a similar $Al_{63.2}Co_{19.5}Cu_{17.3}$ sample by Ribeiro *et al.*[13]

We have analyzed qualitatively the evolution of the LEED patterns as a function of the annealing temperature and of the number of sputter-annealing cycles. Three different annealing temperatures have been used, namely, 973, 1023, and 1073 K. They correspond to 70–80 % of the sample melting point. The background intensity is reduced and diffraction spots become sharper when the number of cycles at a given annealing temperature is increased. This is also verified for increasing annealing temperature. However, we found that surface preparation at 1073 K leads to incomplete terraces as seen by STM, which may indicate the onset of some desorption of surface atoms. Therefore, the maximum annealing temperature used in the following is 1023 K. Finally, we found that one of the samples used in our experiments (sample A1) degraded progressively after several months of use (i.e., a large number of sputter-annealing cycles). The degradation was manifest in the appearance of cracks at the surface. This observation is consistent with the decomposition process of d-Al-Cu-Co single crystals upon long anneal-

ing, reported elsewhere,[25] and is interpreted to be a consequence of the Al-Cu-Co phase diagram (i.e., the composition range of thermodynamic stability of the decagonal phase shifts and widens as the temperature increases).

The twofold surface of d-Al-Cu-Co was further investigated by STM. We summarize here the results obtained using the two different samples of the same composition. Figure 3(a) shows a three-dimensional (3D) representation of a typical STM image recorded on the clean twofold Al-Cu-Co surface annealed at 973 K. It shows flat terraces separated by steps of various heights. The average terrace width is found to depend on the thermal history of the sample. In particular, longer annealing cycles seem to correlate with larger terraces. The line profile shown in Fig. 3(b) is measured along the path indicated by the white line drawn in Fig. 3(c). It shows some of the most frequently measured step heights 0.47, 0.77, 1.24, and 2.07 nm (± 0.05 nm). Smaller step heights are observed additionally, such as 0.19 and 0.30 ± 0.05 nm, and also larger ones corresponding to the bunching of smaller steps. The ratio between two consecutive step heights is close to the golden mean ($\tau = (1 + \sqrt{5})/2 = 1.618…$). Therefore, all the different step heights H can be written as a linear combination of the two smallest steps S and L: $H = mL + nS = (m\tau + n)S$, with ($m,n$) integers and $L/S = \tau$. The smallest step heights are 0.19 and 0.3 nm, but they appear at a very low frequency and they border small terraces. Therefore a more natural choice is to define $S = 0.47$ nm and $L = 0.77$ because these two step heights are more common and delineate larger terraces and are thus associated with more stable surface terminations. These step height values are larger than typical interplanar distances in crystals and hence should correspond to blocks of several layers. These blocks of layers of thickness S and L appear to be stacked along the surface normal according to a Fibonacci sequence, as expected along the quasiperiodic [10000] axis. For example, the line profile shown in Fig. 3(b) can be ascribed from bottom to top to the sequence L-S-L-(LS)-(LSL)-(SL)-S-S, which is part of the Fibonacci sequence generated by the substitution rules $S \rightarrow L$ and $L \rightarrow LS$. However, this stacking sequence contains a defect, as two consecutive S blocks are forbidden in a true Fibonacci sequence. This defect can be ascribed to a planar row of
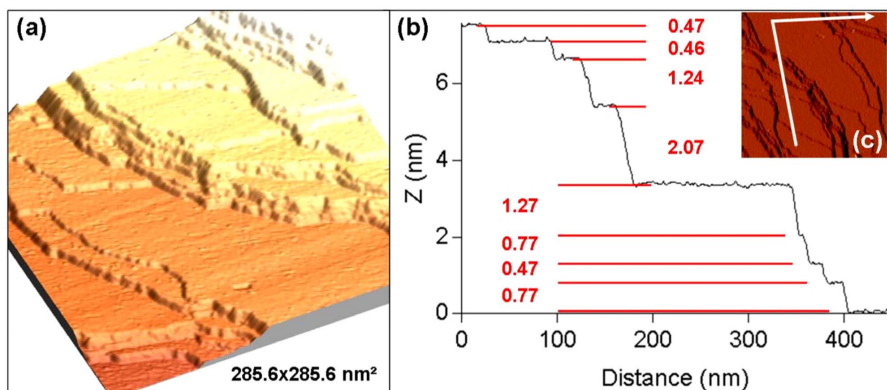

FIG. 3. (Color online) (a) 3D representation of an STM image (285.6×285.6 nm^2) of the clean twofold surface of the d-Al-Cu-Co sample prepared by sputter-annealing (973 K) cycles (-0.8 V and 0.23 nA). (b) Line profile across step edges following the path indicated in (c).

Sample A1 (total = 9 µm²)	
Terrace height (nm)	Area (%)
0.47 ±0.05	15 ±1
0.77 ±0.05	19 ±1
1.25 ±0.05	25 ±1
2.01 ±0.05	14 ±1
3.20 ±0.20	1 ±1

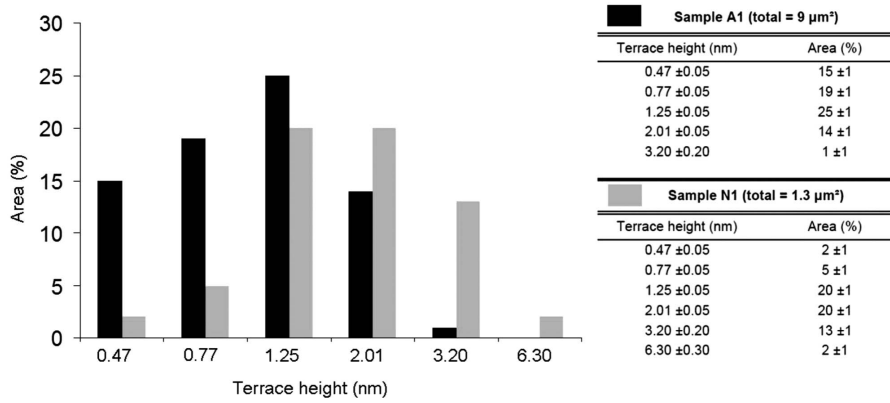| Sample N1 (total = 1.3 µm²)	
Terrace height (nm)	Area (%)
0.47 ±0.05	2 ±1
0.77 ±0.05	5 ±1
1.25 ±0.05	20 ±1
2.01 ±0.05	20 ±1
3.20 ±0.20	13 ±1
6.30 ±0.30	2 ±1

FIG. 4. Percentage of the surface area covered by terraces associated with specific step heights. The results are given for the two samples A1 and N1 annealed at 1023 K but for different times (A1 longer than N1). The total surface area investigated is written in brackets in the table.

phason defects, corresponding to correlated phasonic rearrangements that collectively produce the flipping of two or more blocks of planes along the [10000] direction. Indeed, phason disorder has been reported in this system and manifestations of this disorder are expected also at the surface. We will see later that phason disorder can also be identified within the (10000) surface along the quasiperiodic [001$\bar{1}$0] direction.

Further considerations of STM images indicate a selection mechanism among the different terraces. For example, we frequently observe large terraces separated by a bunch of very narrow terraces which do not really form as stable features. More quantitatively, we have measured the area associated with each of the terraces and labeled them according to their downward step. We repeated these measurements using a large number of STM images. In some cases, parts of the images must be disregarded, especially when they comprise an area where very narrow terraces bunch together. We only take into account STM images that have been acquired using the same surface preparation method in the two sets of experiments, using both samples A1 and N1 prepared at 1023 K, but using different annealing time. A total of 9 µm² was analyzed on the A1 surface, within which 74% of the area was quantified. On N1 sample, only 62% of the 1.3 µm² was quantitatively analyzed, due to more frequent occurrence of regions comprising narrow terraces.

The results listed in Fig. 4 indicate clear differences between both samples. For sample A1, *S*, *L*, and (*LS*) steps are the most populated (0.47, 0.77, and 1.25, nm, respectively). The distribution is shifted toward higher values for sample N1, for which (*LS*), (*LSL*), and (*LSLSL*) are the most populated steps (1.25, 2.01, and 3.20 nm, respectively). As mentioned above, both samples were prepared by annealing at 1023 K, but the annealing time was approximately three times longer for A1 sample. This prolonged annealing period also resulted in larger terraces.

The two sets of observations seem contradictory. On one hand, longer annealing time should facilitate the equilibration of the surface and one expects that the most stable terminations form large terraces. This suggests that A1 corresponds to a more stable surface morphology. On the other hand, step bunching can be a mechanism by which the most

stable planes can be selected as surface terminations in alloy surfaces.[26] The shift in the step-height distribution toward larger values for sample N1 suggests that N1 may be a more stable surface morphology, in contradiction with the previous statement. Other external factors may also have some influence, like the magnitude of the miscut of the single crystals with respect to the [10000] direction, the kinetics of terrace formation, and the long-term history of sample preparation. Nevertheless, the common feature that emerges from Fig. 3 is that step sequences and step-height distributions are consistent with the quasiperiodic stacking of blocks of layers having thicknesses *S* = 0.47 nm and *L* = 0.77 nm, or a combination of these heights.

We will now use this experimental result to identify the nature of the planes selected as surface terminations by using the bulk-structure model presented previously. Figure 5 is a projection of a $10 \times 10 \times 6$ nm³ slab of the model showing the stacking of atomic layers along the quasiperiodic [10000] direction, i.e., the stacking of atomic layers perpendicular to the surface plane. The horizontal direction is either the [001$\bar{1}$0] quasiperiodic direction (left side) or the [00001] periodic direction (right side). Along the [10000] axis, layers of various density and chemistry can be distinguished. A closer inspection reveals that interlayer spacings take different values. The largest values for the interlayer distance gaps are 0.13 and 0.10 nm. The positions of these gaps along the [10000] axis are indicated by arrows in Fig. 5. In between the gaps lie blocks of layers having thicknesses that match very closely the measured step heights *S* = 0.47 and *L* = 0.77 nm. A few blocks of thickness equal to 0.29 nm are also found in the model. The good match between step heights and block thicknesses suggests that the surface preferentially forms at these gaps, which separate more closely spaced atomic layers. Similar phenomena have been observed in icosahedral Al-Pd-Mn and Al-Cu-Fe quasicrystals.[27–32] In these systems, step heights and step sequence along the fivefold axis can also be explained, using bulk-structural models, by the quasiperiodic stacking of blocks of layers separated by gaps and having two different thicknesses. The surface is found to form preferentially at these gaps, exposing atomic planes characterized by a high-density and an Al-rich chemical composition, without any
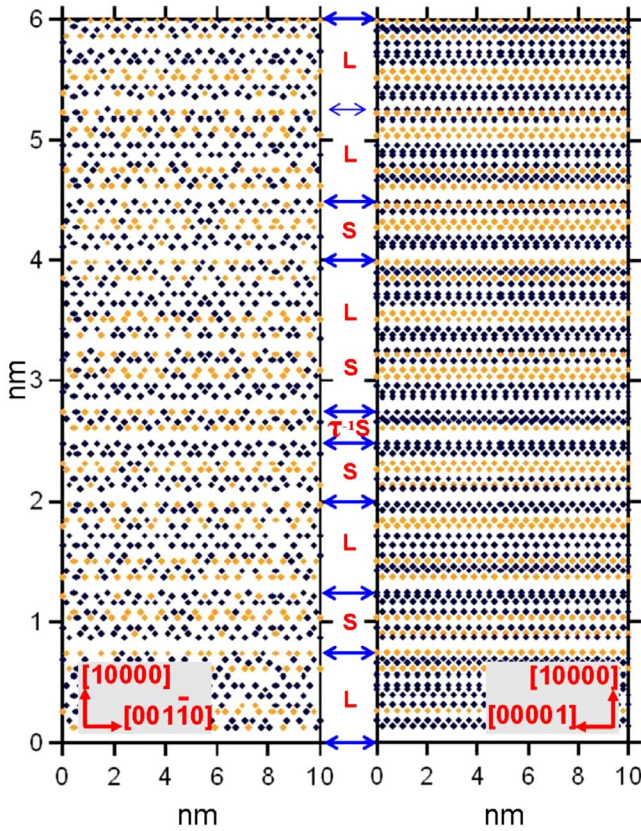
FIG. 5. (Color online) Cross sections of the model oriented along the $[10\overline{0}00]$ direction. The horizontal direction is either the aperiodic $[001\overline{1}0]$ direction (left) or the periodic $[00001]$ direction. The dark (blue) and bright (orange) dots correspond to Al and TM atoms, respectively. The position of gaps separating blocks of layers are indicated by arrows. The gap width is 0.13 nm except for the one indicated by a thin arrow (0.10 nm). Most blocks have a thickness of either $S=0.47$ or $L=0.77$ nm and are stacked according to a Fibonacci sequence.

surface reconstruction or chemical segregation. The same conclusion was reached for the (10000) surface of the d-Al-Ni-Co.[7] In Fig. 1, which shows a section of the model perpendicular to the 10-fold axis, we have outlined one set of densely packed atomic rows running perpendicular to one of the $\langle 10000\rangle$ directions. These dense atomic rows correspond to the block terminations and hence are spaced by either $S=0.47$ or $L=\tau.S=0.77$ nm following a Fibonacci sequence. The lines show the position of surface terminations with respect to the cluster units. We see that columnar clusters can only be truncated by (10000) surface planes at specific positions.

We will now compare high-resolution STM images obtained on various terraces with specific layers of the bulk model that are likely to appear as surface termination. Theses specific layers are the top regions of the S and L blocks identified along the $[10000]$ direction. We use a $10 \times 10 \times 10$ nm^3 slab of the model and generate all possible surface terminations, taking into account all atomic positions within 0.11 nm from the top of the blocks. This particular choice of roughness is supported by two facts. First, it matches the experimental roughness measured by STM on individual ter-

races and second, it leads to realistic surface-atom density. The generated terminations have an average density of 10.6 atoms per nm^2 and an average Al content of 72%. Some of the layers are pure Al while others are mixed Al-TM planes.

It has to be mentioned that similar gaps also exist along the $[001\overline{1}0]$ direction. They define blocks of layers of thicknesses 0.25 and 0.40 nm stacked according to a Fibonacci sequence. These values do not match the experimental step heights. The surface terminations defined by the blocks have an average density of 8.8 atoms per nm^2 and an average Al content of 59% only. All terminations along this direction contains from 30% to 45% of TM atoms. Faceting of the $(001\overline{1}0)$ twofold surface has been reported for an Al-Ni-Co decagonal quasicrystal.[33] Facets appear at $\pm 18°$ from the surface normal where (10000)-equivalent planes are located, thus suggesting that the (10000) planes are more stable than $(001\overline{1}0)$. This is consistent with the fact that possible surface terminations along $[001\overline{1}0]$ are characterized by a lower atomic density and a higher content of TM atoms, both of which will contribute to a higher surface energy compared to (10000) terminations.

Experimentally, we observed three main families of terraces at the (10000) surface of d-Al-Cu-Co. Representative STM images of each type of terrace are shown in Fig. 6 (type I and type II) and Fig. 7 (type III). The first two types [Figs. 6(a) and 6(b)] do not show any bias dependence in the STM contrast. Both surfaces consist of periodic rows aperiodically spaced along the $[001\overline{1}0]$ direction. The period along the $[00001]$ direction is either 0.4 or 0.8 nm depending on the row considered, both periods coexisting on the surface. The spacing between periodic rows is close to $S=0.47$ and $L=0.77$ nm and follows the Fibonacci sequence. In addition to these generic features, the surface contains many defects such as vacancies (dark contrast) and groups of adatoms (bright contrast) lying ~ 0.25 nm above the atomic rows. These adatoms presumably form part of the next layer up. Among the various possible terminations extracted from the bulk model, subsets sharing common features can be found that compare well with each type of terrace. Representative examples of bulk planes presenting a good match are superimposed on STM images for both type-I and type-II terraces in Fig. 6. The size of atoms in the model is a decreasing function of their position below the surface. We see that only the topmost atomic rows contribute significantly to the STM contrast. These atomic rows represent about 30–40 % of the atom density contained within the 0.11-nm-thick block termination for terraces of type I and type II. The spacing between these atomic rows and their sequence match very well with the experiment. We note that both terminations are quite dense (~ 10 atoms/nm^2) and are almost (or totally) pure Al planes ($\sim 100\%$ for type I and 85% for type II). This is consistent with the fact that these two types of terraces do not show any bias dependence in the STM contrast. In addition, by comparing the selected planes and the images, we note that defects like rows of adatoms [Fig. 6(a)] or part of the surface presenting the 0.8 nm periodicity [Fig. 6(b)] are located preferentially in between atomic rows separated by the largest distance (~ 1.3 nm). The space between these atomic rows defines a line of low density, which is energetically unfavorable. Our observations suggest that this situa-
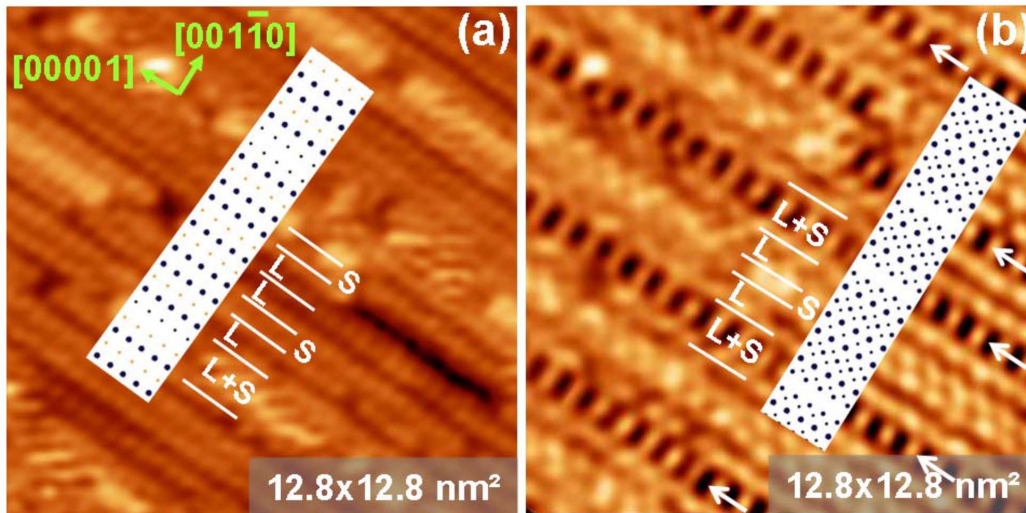
FIG. 6. (Color online) High-resolution STM images (12.8×12.8 nm^2) of terraces of (a) type I and (b) type II (-1 V and 0.5 nA). Atomic rows run along the periodic [00001] direction and are spaced by a distance of either $S = 0.47$ or $L = 0.77$ nm or a combination of both. The periodicity along the rows is 0.4 nm except for those indicated by white arrows in (b) where a doubling of the periodicity is measured. A section of the atomic structure of a representative bulk termination is superimposed on the image for both types of terraces. The dark (blue) and bright (orange) dots correspond to Al and TM atoms, respectively.

tion is circumvented by either a surface reconstruction (0.8 nm periodic lines) or by adsorption of intrinsic adatoms during the surface preparation. In general, these low-density lines are expected to be strong adsorption sites. We emphasize that both terminations of type I and type II share similar characteristics and differ only by their TM content. Thus we cannot unambiguously ascribe terraces of the type shown in Fig. 6(a) to type I or type II and vice versa for terraces of the type shown in Fig. 6(b).

The third type of terrace is shown in Fig. 7. It exhibits a strong bias dependence. Atomic rows with bright contrast in the STM image in Fig. 7(a) are separated by about 1.3 ± 0.1 nm ($\sim LS$) or 2.1 ± 0.1 nm ($\sim LSL$) and follow a Fibonacci sequence along the [001$\bar{1}$0] direction. The periodicity measured on terraces of type III is 0.8 nm along all atomic rows. In between two bright lines separated by 2.1 nm in Fig. 7(a), we observe additional atomic rows of lower contrast for negative bias, i.e., when occupied states of the
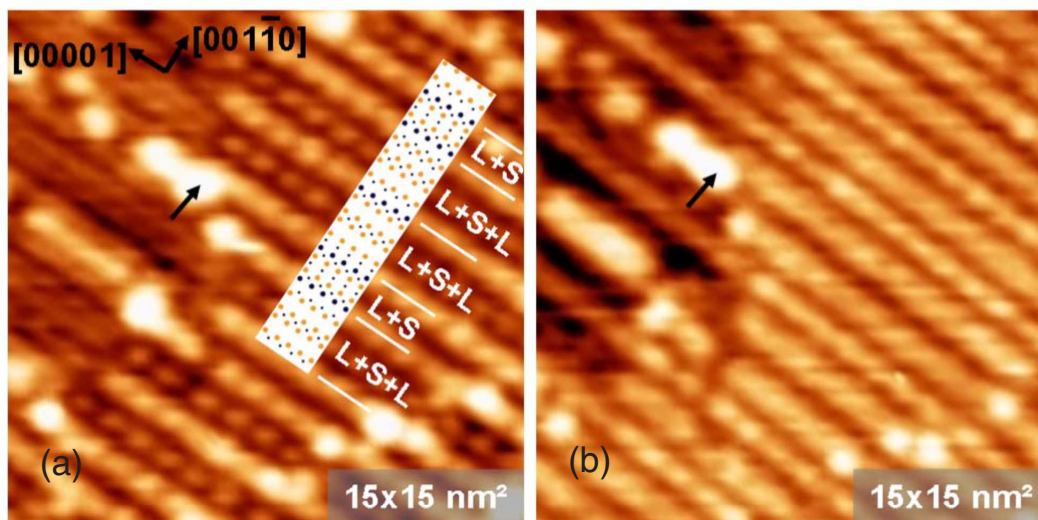

FIG. 7. (Color online) High-resolution STM images (15×15 nm^2) for terraces of type III acquired at negative bias [occupied states probed in (a), (-1.2 V and 0.5 nA)] or at positive bias [unoccupied states probed in (b), (1.2 V, 0.5 nA)]. Atomic rows running along the periodic [00001] direction have a periodicity of 0.8 nm. Rows with bright contrast in (a) are spaced by distances roughly corresponding to $LS \sim 1.3$ nm or $LSL \sim 2.1$ nm. The contrast of atomic rows located in between two bright lines spaced by LSL in (a) increases when tunneling into empty states as in (b). The black arrows indicate the position of the same defect in (a) and (b) as a reference point. A section of the atomic structure of representative bulk termination is superimposed on the image for both types of terraces. The dark (blue) and bright (orange) dots correspond to Al and TM atoms, respectively.

surface are probed. The contrast of these particular atomic rows increases while scanning at positive bias, i.e., when unoccupied states are probed [Fig. 7(b)]. Thus two bright atomic rows separated by 2.1 nm at negative bias transform into three bright rows, each separated by about 1.05 ± 0.1 nm at positive bias. Therefore the resulting sequence of bright rows is based on two distances (1.05 and 1.3 nm) that follows an aperiodic sequence. Because these two distances are quite similar, STM images recorded at positive bias give an impression of periodicity [Fig. 7(b)], although the surface is aperiodic. The bias dependency suggests that terraces of type III contain TM atoms whereas the first two types were almost pure Al. Indeed, TM atoms have localized d-like states that produce sharp features in the electron density of states just around the Fermi level, which can affect drastically the tunneling current in STM. In the decagonal Al-Cu-Co quasicrystal, the Co d band is centered at about -0.7 eV below the Fermi level, while the Cu d band lies further below at about -4 eV.[34–36] Band-structure calculations performed for realistic approximants can reproduce such experimental features and indicate that unoccupied Co d-like states exist above E_F while the Cu d band is almost fully occupied. Atomically resolved STM images of terraces of type III have been compared to the set of all possible generated terminations from the model. As for terraces of type I and type II, we found that a subset of terminations can reasonably account for the experimental observations. A representative example of such terminations is shown in Fig. 7(a). It suggests that rows whose contrast does not change with the bias in STM are either a single row of pure Al or consist of two Al and TM atomic rows separated by 0.3 nm. The bias-dependent atomic rows are identified as double TM lines spaced by 0.3 nm. Terminations corresponding to terraces of type III have a density of about 11 atoms/nm^2 and contain about 40–50 % of TM atoms. The areal occupancy covered by terraces of type III has been estimated from STM images and is lower than 20%. This type of surface termination containing TM atoms is thus the least frequent one. As for terraces of type I and type II, atoms imaged by STM represent only a fraction of all atomic positions contained within the 0.11-nm-thick block termination. The occurrence of the 0.8 nm periodicity cannot be accounted for by the model which only includes the basic 0.4 nm periodicity. In principle, the 0.8 nm periodicity could arise from either a geometrical reconstruction or chemical ordering. Indeed, Cockayne and Widom[20] have proposed a model for the decagonal Al-Cu-Co quasicrystal in which Cu and Co atoms alternate forming zigzag chains extending along the periodic direction. Since the local density of states around Co and Cu atoms is expected to differ, such chemical ordering could explain the superstructure. Within this scenario, one has to consider that atomic rows with no bias dependence consist of two Al and TM atomic rows and not just one pure Al chain. This suggests that the superstructure may originate from a chemical ordering between Cu and Co atoms along the periodic axis. Such chemical ordering is not taken into account in the structure model because x-ray form factors of Cu and Co are nearly equal and cannot be distinguished by x-ray diffraction. We also note that a high content of TM atoms at the surface is energetically unfavorable and so the 0.8 nm periodicity on these planes could also result from a surface reconstruction to decrease the TM content of the top plane and hence the surface energy associated with terraces of type III. Kishida et $al.$[5] have observed similar double and also triple periodicities along atomic rows on the (10000) surface of an Al-Ni-Co decagonal phase, which was attributed to a surface reconstruction.

Finally, we mention that phasonlike defects within the {10000} planes have a relatively high density on the Al-Cu-Co compared to previous reports. The density of interlayer phason defects on the (10000) twofold surfaces of a Co-rich d-Al-Ni-Co has been estimated by Kishida et $al.$[5] from STM images and was found to be very low (2.10^{-4} nm^{-2}). Other observations of surface defects include inversion in the sequence of high-density lines within the fivefold plane of icosahedral quasicrystals.[37] Related phason defects have been reported by Ebert et $al.$[38] in a one-dimensional quasiperiodic superstructure of a thin Ag film on GaAs(110) surfaces. The Ag films exhibits height modulation related to interfacial strain accommodation. This leads to
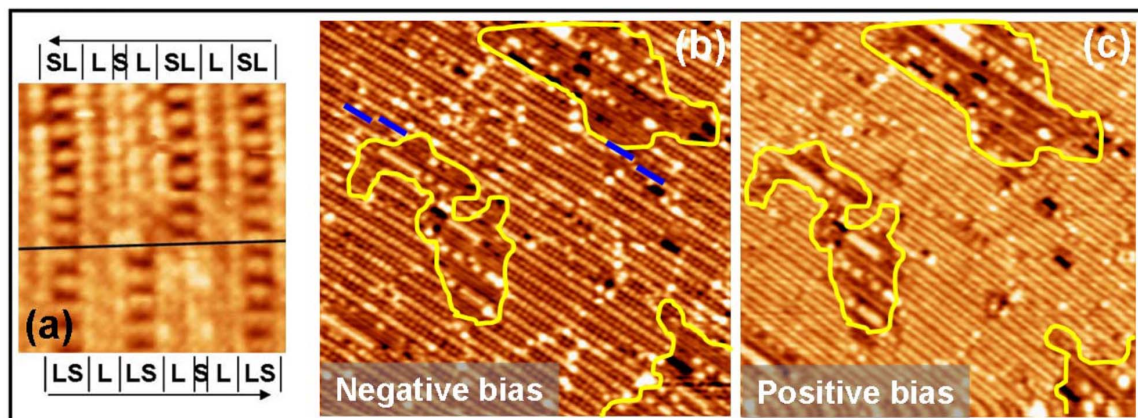

FIG. 8. (Color online) (a) Interlayer phason defect observed on terrace of type I (7.9×7.9 nm^2). (b) and (c) are STM images of the same area (50×50 nm^2) and correspond to a terrace of type III recorded at negative bias [(b), (-1.2 V and 0.5 nA)] or at positive bias [(c), (1.2 V and 0.5 nA)]. Dark (blue) sticks in (b) show inversion in the stacking sequence of the bright lines. While most of the surface area is bias dependent, the part of the surface delimited by the bright (yellow) contour is not.

the formation of stripes separated by two basic distances L and S that follow a Fibonacci sequence, containing dislocations surrounded by phason defects with a concentration estimated at 10^{-2} nm^{-2}. The different types of interlayer phason defects observed on the (10000) d-Al-Cu-Co surface are shown in Fig. 8 for terraces of type I [Fig. 8(a)] and type III [Fig. 8(b)]. They correspond to phason flips between adjacent layers along the aperiodic $[001\bar{1}0]$ direction. Another type of defect is shown in Fig. 8(c). It shows the same image as in Fig. 8(b) but recorded at positive bias. This particular terrace belongs to type III and therefore its STM contrast is bias dependent. However, part of the surface area does not show the same bias dependency, indicating that its chemical nature differs from the rest of the terrace. It may be also attributed to interlayer phason defects but occurring between adjacent layers along the surface normal. This would correspond to the correlated phasonic rearrangements flipping planes or blocks of planes along the [10000] already mentioned earlier. These correlated planar defects are sometimes referred to as "phason wall" and have been observed for example in the icosahedral Al-Pd-Mn quasicrystalline phase.[39]

IV. CONCLUSION

We have investigated the (10000) twofold surface of an Al$_{63.2}$Co$_{19.5}$Cu$_{17.3}$ decagonal phase by LEED and STM. A clean and well-ordered surface can be prepared by sputter annealing. The surface exhibits a terrace and step morphology. Diffraction patterns confirmed the quasiperiodic nature of the surface along the $[001\bar{1}0]$ direction and revealed a weak 0.8 nm superstructure in addition to the basic 0.4 nm periodicity along the [00001] direction. The 0.8 nm superstructure was also observed by STM on specific terraces containing transition-metal atoms. It is attributed to either a surface reconstruction or to an effect of the chemical ordering between Cu and Co atoms along the periodic direction. Three different types of terraces have been identified by STM separated by steps of various heights. We have used the bulk-structure model developed by Deloudi and Steurer[16] and could successfully explain most of all our experimental observations. The measured step heights correspond to thicknesses of blocks of layers separated by gaps in the bulk model. They take values $S = 0.47$ and $L = 0.77$ nm or $H = (m\tau + n)S$, with (m, n) integers and $L/S = \tau$. These S and L blocks are quasiperiodically stacked along the surface normal, in agreement with the observed step sequence. The top regions of the S and L blocks is defined as a termination, taking into account all atomic positions within 0.11 nm from the top of the blocks. We identify three different types of terminations using the bulk model. All have an atomic density of 10–11 at./nm^2 but differ in their chemical composition. Terminations of type I and type II are almost pure Al (from 85% to 100% of Al), while termination of type III contain up to 40–50 % TM atoms. These bulk terminations can be used to interpret the three different types of terraces identified by high-resolution STM. The first two types, characterized by high Al content, do not show any bias dependence in STM, while the third type containing TM atoms is strongly bias dependent. The only feature which cannot be explained by the model is the 0.8 nm superstructure observed on terraces of type III and along specific atomic rows of type II. The reconstructed areas appear to correlate with low-density lines within the surface termination and therefore reconstruction can be viewed as a mechanism to overcome this energetically unfavorable situation. Finally, we have observed a high density of interlayer phason defects corresponding to phason flips of atoms both along the in-plane $[001\bar{1}0]$ direction and along the surface normal. This high density of phason defects directly observed at the surface is a specific feature of the Al-Cu-Co decagonal quasicrystal, as these types of defects have only been rarely observed in other related systems. This fact suggests that the configurational entropy associated with phason disorder is important in this system.

*Present address: Universidade Federal do ABC, Centro de Ciências Naturais e Humanas, Rua Santa Adélia 166 Bangu, 09210-170 Santo Andre, SP, Brazil.

[1] Lin Shu-yuan, Wang Xue-mei, Lu Li, Zhang Dian-lin, L. X. He, and K. X. Kuo, Phys. Rev. B **41**, 9625 (1990).

[2] S. Martin, A. F. Hebard, A. R. Kortan, and F. A. Thiel, Phys. Rev. Lett. **67**, 719 (1991).

[3] J. Y. Park, D. F. Ogletree, M. Salmeron, R. A. Ribeiro, P. C. Canfield, C. J. Jenks, and P. A. Thiel, Science **309**, 1354 (2005).

[4] J. Y. Park, D. F. Ogletree, M. Salmeron, R. A. Ribeiro, P. C. Canfield, C. J. Jenks, and P. A. Thiel, Phys. Rev. B **74**, 024203 (2006).

[5] M. Kishida, Y. Kamimura, R. Tamura, K. Edagawa, S. Takeuchi, T. Sato, Y. Yokoyama, J. Q. Guo, and A. P. Tsai, Phys. Rev. B **65**, 094208 (2002).

[6] H. R. Sharma, K. J. Franke, W. Theis, A. Riemann, S. Fölsch, K. H. Rieder, and P. Gille, Surf. Sci. **561**, 121 (2004).

[7] J. Y. Park, D. F. Ogletree, M. Salmeron, R. A. Ribeiro, P. C. Canfield, C. J. Jenks, and P. A. Thiel, Phys. Rev. B **72**, 220201(R) (2005).

[8] L. X. He, Z. Zhang, Y. K. Wu, and K. H. Kuo, Inst. Phys. Conf. Ser. **2**, 501 (1988).

[9] B. Grushko, Mater. Trans., JIM **34**, 116 (1993).

[10] B. Grushko, Phase Transitions **44**, 99 (1993).

[11] C. Dong, J. M. Dubois, M. De Boissieu, and C. Janot, J. Phys.: Condens. Matter **3**, 1665 (1991).

[12] A. R. Kortan, F. A. Thiel, H. S. Chen, A. P. Tsai, A. Inoue, and T. Masumoto, Phys. Rev. B **40**, 9397 (1989).

[13] R. A. Ribeiro, S. L. Bud'ko, F. C. Laabs, M. J. Kramer, and P. C. Canfield, Philos. Mag. **84**, 1291 (2004).

[14] Y. Yokoyama, R. Note, A. Yamaguchi, A. Inoue, K. Fukaura, and H. Sunada, Mater. Trans., JIM **40**, 123 (1999).

[15] G. Meistererernst, L. Zhang, P. Dreier, and P. Gille, Philos. Mag. **86**, 323 (2006).

[16] S. Deloudi, Ph.D. thesis, ETH, Zürich, 2008.

[17] W. Steurer and K. H. Kuo, Acta Crystallogr., Sect. B: Struct. Sci. **46**, 703 (1990).

[18] S. E. Burkov, Phys. Rev. Lett. **67**, 614 (1991); Phys. Rev. B **47**, 12325 (1993).

[19] R. F. Sabiryanov, S. K. Bose, and S. E. Burkov, J. Phys.: Condens. Matter **7**, 5437 (1995).

[20] E. Cockayne and M. Widom, Phys. Rev. Lett. **81**, 598 (1998).

[21] I. Al-Lehyani and M. Widom, Phys. Rev. B **67**, 014204 (2003).

[22] W. Steurer, Z. Kristallogr. **219**, 391 (2004).

[23] A. R. Kortan, R. S. Becker, F. A. Thiel, and H. S. Chen, Phys. Rev. Lett. **64**, 200 (1990).

[24] I. Horcas, R. Fernandez, J. M. Gomez-Rodriguez, J. Colchero, J. Gomez-Herrero, and A. M. Baro, Rev. Sci. Instrum. **78**, 013705 (2007).

[25] W. Bogdanowicz, Cryst. Res. Technol. **40**, 482 (2005).

[26] L. Barbier, B. Salanon, and A. Loiseau, Phys. Rev. B **50**, 4929 (1994).

[27] M. Gierer, M. A. Van Hove, A. I. Goldman, Z. Shen, S. L. Chang, P. J. Pinhero, C. J. Jenks, J. W. Anderegg, C. M. Zhang, and P. A. Thiel, Phys. Rev. B **57**, 7628 (1998).

[28] T. Cai, F. Shi, Z. Shen, M. Gierer, A. I. Goldman, M. J. Kramer, C. J. Jenks, T. A. Lograsso, D. W. Delaney, P. A. Thiel, and M. A. VanHove, Surf. Sci. **495**, 19 (2001).

[29] Z. Papadopolos, G. Kasner, J. Ledieu, E. J. Cox, N. V. Richardson, Q. Chen, R. D. Diehl, T. A. Lograsso, A. R. Ross, and R. McGrath, Phys. Rev. B **66**, 184207 (2002).

[30] L. Barbier, D. Le Floc'h, Y. Calvayrac, and D. Gratias, Phys. Rev. Lett. **88**, 085506 (2002).

[31] H. R. Sharma, V. Fournée, M. Shimoda, A. R. Ross, T. A. Lograsso, A. P. Tsai, and A. Yamamoto, Phys. Rev. Lett. **93**, 165502 (2004).

[32] B. Unal, T. A. Lograsso, A. Ross, C. J. Jenks, and P. A. Thiel, Phys. Rev. B **71**, 165411 (2005).

[33] K. J. Franke, Ph.D. thesis, Freie University, 2003.

[34] G. Trambly de Laissardière and T. Fujiwara, Phys. Rev. B **50**, 9843 (1994).

[35] M. Krajci, J. Hafner, and M. Mihalkovic, Phys. Rev. B **56**, 3072 (1997).

[36] E. Belin-Ferré, Z. Dankhazi, V. Fournée, A. Sadoc, C. Berger, H. Müller, and H. Kirchmayer, J. Phys.: Condens. Matter **8**, 6213 (1996); Z. M. Stadnik, G. W. Zhang, A. P. Tsai, and A. Inoue, Phys. Rev. B **51**, 11358 (1995).

[37] T. Cai, V. Fournée, T. Lograsso, A. Ross, and P. A. Thiel, Phys. Rev. B **65**, 140202(R) (2002).

[38] Ph. Ebert, K.-J. Chao, Q. Niu, and C. K. Shih, Phys. Rev. Lett. **83**, 3222 (1999).

[39] M. Feuerbacher and D. Caillard, Acta Mater. **54**, 3233 (2006).